

## Supplementary information

# Modeling Interfacial electrochemistry: concepts and tools

Anja Kopač Lautar<sup>1</sup>, Arthur Hagopian<sup>2,3</sup>, Jean-Sébastien Filhol<sup>\*2,3</sup>

<sup>1</sup>*Department of Materials Chemistry, National Institute of Chemistry, Slovenia*

<sup>2</sup>*Institut Charles Gerhardt, CNRS & Université de Montpellier, Place E. Bataillon, France*

<sup>3</sup>*RS2E French network on Electrochemical Energy Storage, FR5439, Amiens, France*

**\*Corresponding author: Jean-Sébastien Filhol (jean-sebastien.filhol@umontpellier.fr)**

### S0. Detailed derivation for extended CHE approximation.

$$\begin{aligned}\Delta F(V) &= F_{S-H}(V) - F_S(V) - \frac{1}{2}E_{H_2} + e(V - V_{H^+/H_2}) \\ &\approx E_{S-H}^0 - E_S^0 - \frac{1}{2}E_{H_2} + e(V - V_{H^+/H_2}) - \frac{1}{2}C(V - V_{S-H}^0)^2 + \frac{1}{2}C(V - V_S^0)^2 \\ &= E_{S-H}^0 - E_S^0 - \frac{1}{2}E_{H_2} + e(V - V_{H^+/H_2}) + C(V_{S-H}^0 - V_S^0)\left(V - \frac{V_{S-H}^0 + V_S^0}{2}\right)\end{aligned}$$

$$\Delta F(V) \approx E_{S-H}^0 - E_S^0 - \frac{1}{2}E_{H_2} + (1 + \varepsilon)e(V - V_{H^+/H_2}) - \varepsilon e(V_m^0 - V_{H^+/H_2})$$

With  $V_m^0 = \frac{V_{S-H}^0 + V_S^0}{2}$  and  $\varepsilon e = C(V_{S-H}^0 - V_S^0)$ . We can rewrite the last equation into form:

$$\Delta F(V) \approx \Delta F_{CHE}(V) + \varepsilon e(V - V_m^0) \approx \Delta F_{CHE}(V) + C(V_{S-H}^0 - V_S^0)(V - V_m^0)$$

### S1. Corrections to homogeneous background method due to introduction of the background charge.

The inclusion of the background charge distributed homogeneously across the entire unit cell requires a couple of corrections to the computed DFT energy.<sup>1,2</sup>

The interaction of the homogeneous background with the charged system gives a non-physical chemical potential that contributes to the energy computed via DFT. This can be a source of large errors and energy correction is necessary.<sup>2</sup> As the charge of the homogeneous background is exactly the opposite than the charge of excess electrons, it holds that:

$$N_{bg} = N_e \quad (1)$$

Where  $N_e$  and  $N_{bg}$  are the numbers of added/withdrawn electrons and of background charges, respectively. The differential of the total computed energy can be written as:

$$dE_{DFT}(N_e) = \tilde{\mu}_e dN_e + \tilde{\mu}_{bg} dN_{bg} = (\tilde{\mu}_e + \tilde{\mu}_{bg}) dN_e \quad (2)$$

Where  $\tilde{\mu}_e$  and  $\tilde{\mu}_{bg}$  are the electrochemical potentials of the charged system and the homogeneous background, respectively. The latter can be calculated from its electrostatic interaction with the charged system over the whole unit cell volume  $\Omega$ :

$$\tilde{\mu}_{bg} = \frac{-e_0}{\Omega} \int_{\Omega} V(r, N_e) dr = e_0 V_a(N_e) \quad (3)$$

Where  $V(r, N_e)$  is the electrostatic potential and  $V_a(N_e)$  is the potential averaged over the unit cell.

Substituting **Eq. 3** into **Eq. 2** and taking into account that the real electronic energy is  $E_e = \tilde{\mu}_e N_e$  we get:

$$E_e = E_{DFT}(N_e) + e_0 \int_0^{N_e} V_a(N) dN \quad (4)$$

Another correction is needed due to a non-physical bulk charge in the metal slab that is induced by the homogeneous background. The bulk charge in the metal slab is neutralized by using a fraction of the added/withdrawn electrons to screen the background charge, meaning that this specific fraction of added/withdrawn electrons is not used for the surface charging, i.e. not for the tuning of the potential

of the system.<sup>2</sup> To make a correction of this effect, the charging of the system is decomposed into electrochemical part arising from the active charge used for the tuning of the potential  $N_{active}$  and a non-physical bulk metal charge  $N_{bulk}$ :<sup>2</sup>

$$\mu_e dN_e = \mu_e (dN_{active} + dN_{bulk}) = dE_{DFT} + \mu_b dN_e \quad (5)$$

where the last equality was obtained using **Eq. 2**. As the average charge in the metal slab has to be zero, the fraction of the background charge in the metal is neutralized by a fraction of the added/withdrawn electrons. If the vacuum size is  $d_0$ , the fraction of the added/withdrawn electrons needed to keep the bulk uncharged can be estimated by considering the entire unit cell size  $d$  in comparison to that of the metal  $d - d_0$ :

$$N_{bulk} \approx \frac{N_e (d - d_0)}{d} \quad (6)$$

The number of electrons used to charge the system is then:

$$N_{active} = N_e - N_{bulk} \approx \frac{N_e d_0}{d} \quad (7)$$

The physically meaningful energy comes from the surface charging:

$$dE_{corr} = \mu_e dN_{active} \approx \frac{d_0}{d} \mu_e dN_e = \frac{d_0}{d} (dE_{DFT} + \mu_{bg} dN_e) \quad (8)$$

Integration gives:

$$E_{corr} - E_{DFT}^0 = \frac{d_0}{d} \left( \int_0^{N_e} dE_{DFT} + \int_0^{N_e} \mu_{bg} dN \right) \quad (9)$$

The final energy correction is obtained by using the **Eq. 3** and rearranging:

$$E_{corr} = E_{DFT}^0 + \frac{d_0}{d} (E_{DFT}(N_e) - E_{DFT}^0 + e_0 \int_0^{N_e} V_a(N) dN) \quad (10)$$

## S2. Computational details.

Periodic DFT calculations were performed using the Vienna *Ab Initio* Simulation Package (VASP)<sup>3,4</sup> within the generalized gradient approximation (GGA) using PBE<sup>5</sup> functional for exchange and correlation potential and projector augmented wave pseudopotentials (PAW)<sup>6</sup> with a cut-off energy of 450 eV. Long-range electrostatic interactions between interfaces arising from periodic boundary conditions were avoided by building a symmetric unit cell. For magnesium calculations, the electrode surfaces were modelled with a 5-layer symmetric slab of Mg (0001) surface in a (5 x 5) supercell. One Mg<sup>2+</sup> solvated cation with explicit solvent molecules was added at each side of the slab (**Figs. S1a and S1b**) symmetrically. This ensured a homogeneous charging of both sides of the slab for the electrochemical calculations to coherently extract the energetic of the charge interfaces (**Fig. S1c**). The interslab distance between periodic surfaces was set to 40 Å and an implicit solvent was added by means of a Polarizable Continuum Model (PCM) as provided by VASPSOL.<sup>7,8</sup> The PCM is parameterized with the solvent dielectric constant (i.e. DME  $\epsilon_r = 7.20$ ) and the cavity size defined by an electronic density cut-off parameter (**Fig. S1**). The density cut-off parameter was determined as  $2.5 \times 10^{-5}$  for the studied systems. As previously shown,<sup>9</sup> the use of PCM makes the electrochemical properties mostly independent of the vacuum size. The Brillouin zone integration in k-space was performed on a  $4 \times 4 \times 1$  k-point grid. Structural relaxations were performed on all atoms except the central Mg-slab layer, which was kept frozen to bulk parameters. The residual forces after structural relaxation were lower than 0.01 eV/Å and all molecules are allowed to re-orientate without external constrain. Due to the large vacuum layer allowing a clear-cut separation between surface and cation, the surface and solvated cation charges were obtained by direct electron density grid integration.

For platinum calculations, 7-layers symmetric slabs of Pt (111) surface were used. CO molecules were added on top position at each side of the slab. The vacuum width was set to 15 Å. The implicit solvation was defined considering water dielectric constant ( $\epsilon_r = 78.5$ ) and a density cut-off parameter of  $2.5 \times 10^{-4}$ . The Brillouin zone integration in k-space was performed on a  $9 \times 9 \times 1$  k-point grid.

## S3 Potential dependent Fukui function calculation

Potential-dependent Fukui function  $f(V(N_e))$  is computed using the following procedure. The equilibrium structure obtained for a given potential  $V$  associated with a charge  $N_e$  is computed at DFT level and the corresponding charge density grid  $\rho(N_e)$  is extracted. Using the same geometry and a single point calculation, a new charge density grid  $\rho(N_e + \varepsilon)$  is computed by adding a fraction of  $\varepsilon$  electron to the system ( $\varepsilon = 0.1$  in the present calculations). The Fukui function grid is then

extracted by finite difference using 
$$f(V) = \frac{\rho(N_e + \varepsilon) - \rho(N_e)}{\varepsilon} .$$

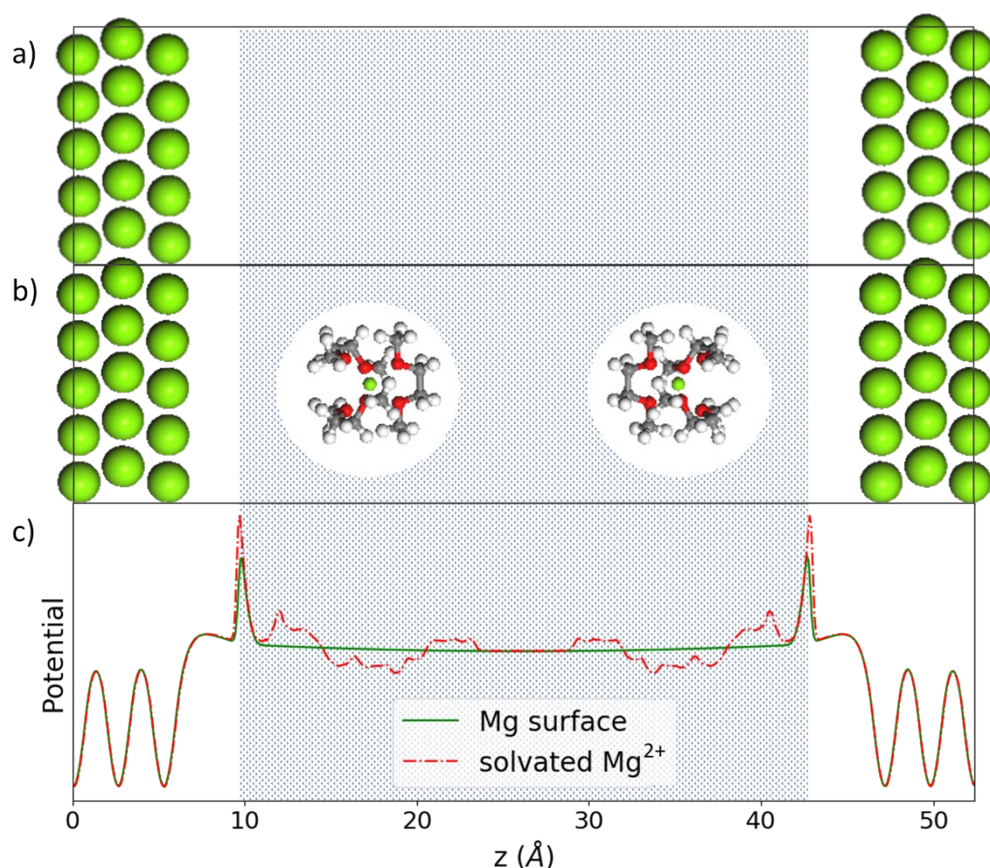


**Figure S1.** (a) Unit cell of a bare magnesium surface (reduced system) and (b) magnesium solvated in monoglyme (oxidized system). (c) Averaged potential over (x,y)-plane for magnesium surface and magnesium solvated in monoglyme at the computed equilibrium potential of the two systems (-2.39 V/SHE = 2.11 V/vacuum). The symmetry of the averaged potential allows unambiguous determination of the vacuum potential and Fermi levels, i.e. the potential of the system. A bump in the averaged potential appearing at approximately 3.5 Å from the surface indicates where PCM starts taking hold. It is tuned by the electronic density cut-off parameter which was set to  $2.5 \times 10^{-5}$  for the studied systems. The shaded region in all three figures is a schematic representation of the region where PCM is taken into account. As the plot is done for equilibrium potential, the Fermi levels of the two systems are aligned. In the calculation for bare surface 0.6 electron was added to shift the system from potential of zero charge to the equilibrium potential, while in solvated Mg calculation 1.6 electrons is subtracted.<sup>1</sup>

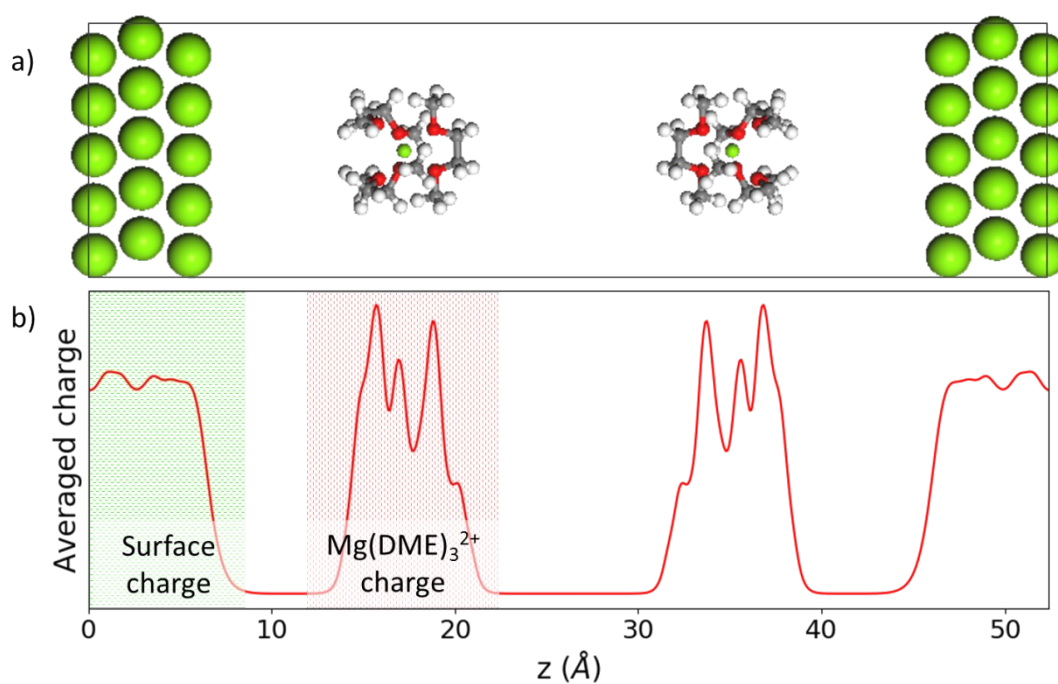


**Figure S2. (a)** Unit cell of  $Mg(DME)_3^{2+}$  system. **(b)** Charge distribution averaged over the  $(x,y)$ -plane in the  $Mg(DME)_3^{2+}$  system. Note that the surface charge and the charge on solvated  $Mg^{2+}$  complex are clearly separated. This allows for unambiguous definition of surface and  $Mg^{2+}$  complex charge via integration of the plotted charge distribution in the region of surface and Mg complex, respectively.<sup>1</sup>

## References

- 1 A. Kopač Lautar, 2019.
- 2 M. Mamatkulov and J. S. Filhol, *Phys. Chem. Chem. Phys.*, 2011, **13**, 7675–7684.
- 3 G. Kresse and J. Furthmüller, *Phys. Rev. B*, 1996, **54**, 11169–11186.
- 4 G. Kresse and J. Furthmüller, *Comput. Mater. Sci.*, 1996, **6**, 15–50.
- 5 J. P. Perdew, K. Burke and M. Ernzerhof, *Phys. Rev. Lett.*, 1996, **77**, 3865–3868.
- 6 G. Kresse and D. Joubert, *Phys. Rev. B*, 1999, **59**, 1758–1775.
- 7 K. Mathew, R. Sundararaman, K. Letchowrth-Weaver, T. A. Arias and R. G. Henning, *J. Chem. Phys.*, 2014, **8**, 084106.
- 8 M. Fishman, H. L. Zhuang, K. Mathew, W. Dirschka and R. G. Hennig, *Phys. Rev. B*, 2013, **87**, 245402.
- 9 N. Lespes and J. S. Filhol, *J. Chem. Theory Comput.*, 2015, **11**, 3375–3382.